

# The unique determination of neuronal currents in the brain via magnetoencephalography

A S Fokas<sup>1</sup>, Y Kurylev<sup>2</sup> and V Marinakis<sup>1</sup>

<sup>1</sup> Department of Applied Mathematics and Theoretical Physics, University of Cambridge, Cambridge CB3 0WA, UK

<sup>2</sup> Department of Mathematical Sciences, Loughborough University, Loughborough, Leics LE11 3TU, UK

Received 31 October 2003, in final form 20 April 2004

Published 21 May 2004

Online at [stacks.iop.org/IP/20/1067](http://stacks.iop.org/IP/20/1067)

DOI: 10.1088/0266-5611/20/4/005

## Abstract

The problem of determining the neuronal current inside the brain from measurements of the induced magnetic field outside the head is discussed under the assumption that the space occupied by the brain is approximately spherical. By inverting the Geselowitz equation, the part of the current which can be reconstructed from the measurements is precisely determined. This actually consists of only certain moments of one of the two functions specifying the tangential part of the current. The other function specifying the tangential part of the current as well as the radial part of the current is completely arbitrary. However, it is also shown that with the assumption of energy minimization, the current can be reconstructed uniquely. A numerical implementation of this unique reconstruction is also presented.

## 1. Introduction

Magnetoencephalography (MEG) is a non-invasive technique that can be used to investigate brain activity. The physiological basis of MEG is the following: the main functional units of the brain are certain highly specialized cells called neurons. For higher mental processes, the most important part of the brain is its outermost layer called cerebral cortex, which contains at least  $10^{10}$  neurons. When neurons are active they produce small currents whose basis is the change in the concentration of certain ions [1] (ionic currents). The flow of current in the neural system produces a weak magnetic field. The measurement of this field outside the brain and the estimation of the current density distribution that produced this field is called MEG. Other names often used are magnetic source imaging, magnetic field tomography and current-flow imaging.

Neuromagnetic signals are typically 50–500 fT, which are of the order of  $10^{-9}$  of the Earth's geomagnetic field. Currently, the only detector that can measure these tiny fields is the

superconducting quantum interference device (SQUID). The theory and practice of SQUID as applied to MEG measurements, as well as several practical approaches for shielding all other external magnetic fields except that of the brain, are discussed in the excellent review [2]. Here, we only note that the SQUID, which is the most sensitive detector of any kind available to scientists [3], is based on the exploitation of several quantum-mechanical effects, including superconductivity as well as the Josephson effect. The SQUID can be thought of as a digital magnetometer where each ‘digit’ represents one flux quantum, and it is essentially a transducer converting a tiny change in magnetic flux into a voltage. Whole-head magnetometer systems are now used by several laboratories in Europe, USA and Japan.

The current density  $\mathbf{J}$  and the magnetic field  $\mathbf{B}$  are related by the Maxwell equations. These equations can be simplified using two facts. First, the permeability of the tissue in the head denoted by  $\mu$  is that of the free space, i.e.  $\mu = \mu_0$ . Second, the quasistatic approximation is valid, namely, the terms  $\partial\mathbf{E}/\partial t$  and  $\partial\mathbf{B}/\partial t$  can be neglected, where  $\mathbf{E}$  denotes the electric field<sup>3</sup>. Using these facts the Maxwell equations become

$$\nabla \cdot \mathbf{B} = 0, \quad \nabla \wedge \mathbf{B} = \mu_0 \mathbf{J}, \quad (1.1)$$

where  $\cdot$  and  $\wedge$  denote the scalar and vector product, respectively, and  $\nabla$  denotes the usual gradient. Part of  $\mathbf{J}$  is due to neuronal activity and part of  $\mathbf{J}$  is due to the electric field  $\mathbf{E}$ ,

$$\mathbf{J} = \mathbf{J}^p + \sigma \mathbf{E}, \quad (1.2)$$

where  $\mathbf{J}^p$  denotes the neuronal current (primary current) and  $\sigma$  denotes the conductivity. The electric field  $\mathbf{E}$  satisfies  $\nabla \wedge \mathbf{E} = \mathbf{0}$ , thus there exists a scalar function  $V$ , called the voltage potential, such that

$$\mathbf{E} = -\nabla V. \quad (1.3)$$

Making the further assumption that  $\sigma = \sigma_I$  inside the head and  $\sigma = \sigma_O$  outside the head, where  $\sigma_O$  and  $\sigma_I$  are constants, equations (1.1)–(1.3) imply the celebrated Geselowitz equation [4]

$$\begin{aligned} \mathbf{B}(\mathbf{x}) = & \frac{\mu_0}{4\pi} \int_{\Omega} \mathbf{J}^p(\mathbf{y}) \wedge \frac{\mathbf{x} - \mathbf{y}}{|\mathbf{x} - \mathbf{y}|^3} d\mathbf{y} \\ & - \frac{\mu_0}{4\pi} (\sigma_I - \sigma_O) \int_{\partial\Omega} V(\mathbf{y}) \mathbf{n}(\mathbf{y}) \wedge \frac{\mathbf{x} - \mathbf{y}}{|\mathbf{x} - \mathbf{y}|^3} dS, \quad \mathbf{x} \notin \Omega, \end{aligned} \quad (1.4)$$

where  $|\mathbf{x}|$  denotes the length of the vector  $\mathbf{x}$ ,  $\Omega$  denotes the volume occupied by the head,  $\partial\Omega$  is the boundary of  $\Omega$ ,  $\mathbf{n}$  denotes the unit outward vector normal to the surface  $\partial\Omega$  and  $dS$  denotes the infinitesimal surface element on  $\partial\Omega$ . For a recent rigorous derivation of this equation see [5].

Equation (1.4) relates  $\mathbf{J}^p$  inside the head with  $\mathbf{B}$  outside the head. However, it also involves the value of  $V$  on the surface of the head. This serious complication can be avoided if one makes the simplifying assumption that the head is spherical. Then, and if in addition  $\sigma_O = 0$ , which is justified since  $\sigma_O \ll \sigma_I$ , equation (1.4) reduces to [6–8]

$$\begin{aligned} \mathbf{B} &= \mu_0 \nabla U, \\ U(\mathbf{x}) &= \frac{1}{4\pi} \int_{|\mathbf{y}| \leq 1} \frac{\mathbf{J}^p(\mathbf{y}) \wedge \mathbf{y} d\mathbf{y}}{|\mathbf{x} - \mathbf{y}| (|\mathbf{x}| |\mathbf{x} - \mathbf{y}| + \mathbf{x} \cdot (\mathbf{x} - \mathbf{y}))} \cdot \mathbf{x}, \quad |\mathbf{x}| > 1. \end{aligned} \quad (1.5)$$

<sup>3</sup> Let  $\sigma$  and  $\varepsilon$  denote conductivity and permittivity which are assumed to be uniform, and let  $\mathbf{E} = \mathbf{E}_0(\mathbf{x}) \exp(2\pi i f t)$ , where  $f$  denotes frequency. Then Maxwell equations imply that the term  $\partial\mathbf{E}/\partial t$  can be neglected provided that  $|\varepsilon \partial\mathbf{E}/\partial t| \ll |\sigma \mathbf{E}|$ , or  $2\pi f \varepsilon / \sigma \ll 1$ . This is indeed the case since for the brain  $\sigma = 0.3 \Omega^{-1} \text{m}^{-1}$ ,  $\varepsilon = 10^5 \varepsilon_0$ , and since in neuromagnetism one usually deals with frequencies of about 100 Hz [2],  $2\pi f \varepsilon / \sigma \sim 2 \times 10^{-3}$ . Similar arguments hold true for the  $\mathbf{B}$  field.

Equation (1.5) relates  $\mathbf{J}^p$  inside the head ( $|\mathbf{x}| < 1$ ) with  $\mathbf{B}$  outside the head. This equation is the starting point of many of the algorithms used in MEG. It defines the following inverse problem: given  $\mathbf{B}$ , which is obtained from the measurements, find  $\mathbf{J}^p$ .

The main difficulty with the above inverse problem is that it is *not* unique. This fact was already known to Helmholtz since 1853 [9]. For example, it is clear from equation (1.5) that the radial part of  $\mathbf{J}^p$  does not contribute to  $U$ . However, in spite of intense scrutiny by many investigators, the fundamental question of *which part of  $\mathbf{J}^p$  can be reconstructed* remained open.

Here we first give a complete answer to this question, see theorem 2:  $\mathbf{J}^p$  can be uniquely decomposed in the form

$$J^\rho \mathbf{e}_\rho + \frac{1}{\rho} \left( \frac{\partial G}{\partial \theta} - \frac{1}{\sin \theta} \frac{\partial F}{\partial \varphi} \right) \mathbf{e}_\theta + \frac{1}{\rho} \left( \frac{1}{\sin \theta} \frac{\partial G}{\partial \varphi} + \frac{\partial F}{\partial \theta} \right) \mathbf{e}_\varphi, \tag{1.6}$$

where  $\mathbf{e}_\rho, \mathbf{e}_\theta, \mathbf{e}_\varphi$  are the unit vectors associated with the spherical coordinates  $(\rho, \theta, \varphi)$  and  $J^\rho, G, F$  are the scalar functions of  $(\rho, \theta, \varphi)$ . This decomposition for vector fields on the sphere is the analogue of the celebrated Helmholtz decomposition for vector fields on  $\mathbb{R}^3$ . We will show that knowledge of  $U$  determines only certain moments of  $F$  with respect to  $\rho$ , while  $J^\rho$  and  $G$  are arbitrary. More precisely, it can be shown that  $U$  can be represented in the form  $U = \sum_{\ell,m} c_{\ell,m} \rho^{-(\ell+1)} Y_{\ell,m}(\theta, \varphi)$ , where  $Y_{\ell,m}$  are the usual spherical harmonics and the constants  $c_{\ell,m}$  are determined from the measurements. Then we will show that  $F$  can be represented in the form  $F = \sum_{\ell,m} f_{\ell,m}(\rho) Y_{\ell,m}(\theta, \varphi)$ , where only the moments of  $f_{\ell,m}$  are determined in terms of  $c_{\ell,m}$ ,

$$\ell \int_0^1 \rho^{\ell+1} f_{\ell,m}(\rho) d\rho = (2\ell + 1) c_{\ell,m}.$$

The above results imply that by decomposing  $\mathbf{J}^p$  into a ‘silent’ component and into an ‘effective’ component, we can show that the Geselowitz integral operator provides a one-to-one map of the effective component of  $\mathbf{J}^p$  into the magnetic field  $\mathbf{B}$ , or into the magnetic potential  $U$ , outside the brain. Furthermore, given  $U$  the effective component can be explicitly computed. We emphasise that, since the decomposition into a silent and into an effective part is of a general nature independent of any assumptions on  $\mathbf{J}^p$ , our result that  $U$  determines the effective component of the current uniquely and says nothing about the silent component, is actually a general statement which is *model independent*.

The next part of the paper deals with the case when we assume some relations between the effective and the silent components: we will show that if one requires that  $\mathbf{J}^p$  is such that energy is minimized, then  $\mathbf{J}^p$  is indeed unique, see theorem 3: in this case  $J^\rho, G, F$  are given by the equations

$$J^\rho = G = 0, \quad F = \sum_{\ell=1}^{\infty} \sum_{m=-\ell}^{\ell} \frac{(2\ell + 1)(2\ell + 3)}{\ell} c_{\ell,m} \rho^{\ell+1} Y_{\ell,m}(\theta, \varphi). \tag{1.7}$$

In addition to the above analytical results we also present a numerical algorithm which given  $U(\rho, \theta, \varphi)$  for one specific value of  $\rho > 1$  and for some equally spaced values  $\{\theta_i\}_0^{i_{\max}}$  and  $\{\varphi_j\}_0^{j_{\max}}$  first computes  $c_{\ell,m}$  and then computes  $\mathbf{J}^p$  using equations (1.6) and (1.7).

The non-uniqueness of the inverse problem has been the Achilles heel of MEG. For example in the most comprehensive review on MEG [2], it is written that ‘with the assumption that MEG mainly reflects the activity in the tangential part of the cortical currents’, while in [10] it is written that ‘what cannot be seen should not be looked for’. Even the ‘father’ of MEG, D Cohen has stated [11], ‘identifying those tangential sources, rather than localization, is the real use of the MEG, there is no localization magic’. We hope that both the analytical

and the numerical results presented here will contribute towards determining the advantages as well as the limitations of MEG.

Regarding other brain imaging techniques we note that at present time the most important such techniques are the functional magnetic resonance imaging (fMRI), the positron emission tomography (PET) and the single photon emission computed tomography (SPECT), as well as a new version of electroencephalography (EEG). These techniques involve trade-offs among the following important considerations: temporal resolution, spatial resolution, invasiveness and cost. Assuming that the question of uniqueness of the MEG is answered, the spatial resolution of MEG (1 cm), of PET and SPECT (4–5 mm) and of fMRI (1.5 mm) are similar; the spatial resolution of the conventional EEG is quite poor. On the other hand, the time resolution of EEG and MEG is much better than that of PET, SPECT and fMRI. The time resolution of PET, SPECT and MRI is of the order of 1 s, while that of MEG and EEG is of the order of 10 ms. This is a crucial factor if one wants to study brain dynamics. For example, MEG data suggest that speech areas of the brain are activated 100 ms after the visual areas. MEG is the only truly non-invasive method. EEG is minimally invasive (placing electrodes on the scalp), while in PET, SPECT and MRI the subject is exposed to radioactive tracers and to strong magnetic fields, respectively. EEG requires a rather inexpensive apparatus (of the order of thousands of dollars). The fMRI has the advantage that can be obtained by modifying the existing MRI apparatus. PET employs positron-emitting radionuclides which have such short half-lives that there must be a cyclotron near the site of scanning, thus the cost is of the order of multimillion dollars. The cost of MEG is similar to that of PET.

We conclude the introduction with some remarks.

- (a) We expect that the combination of our analysis of the spherical model and perturbation theory can be used to study realistic head geometries. In this respect, we also note that progress has been recently made regarding ellipsoidal geometry [12].
- (b) The question of what additional information can one obtain by measuring  $\mathbf{E}$  (using EEG) is under investigation.
- (c) Due to the orthogonality of the decomposition of  $\mathbf{J}^p$  into silent and effective components, the assumption that the  $L^2$  norm of the solution is minimal implies that the silent component vanishes. Clearly, one can assume other relations between the silent and the effective components, for example, one may assume that the current consists of a finite number of dipoles. It is well known that this assumption, under certain conditions, also leads to a unique solution. This current can also be represented in the form (1.6) with  $F$  of a particular form, and therefore can be considered within our formulation. Thus, the answer becomes model dependent only at the stage when one makes an assumption about the form of  $\mathbf{J}^p$ . For other models see [13–15].
- (d) ‘Least-squares’ methods have been used extensively in inverse problems. However, our approach of using such methods in order to find an approximate numerical solution of the Geselowitz equation is fundamentally different from the existing ones. Indeed, it is based on the explicit decomposition of the current into a silent and an effective component, and thus could not have been used before obtaining this decomposition.
- (e) In practice, the magnetic field is measured approximately over a half-sphere over the head and *not* over a whole sphere. However, since in the numerical reconstruction we assume a *finite* number of spherical harmonics, the approximate knowledge of  $U$  over part of a sphere is sufficient to determine approximately the current. Clearly, the problem becomes more and more ill-posed when the number of spherical harmonics increases. A stability result in this direction is under investigation.
- (f) It has been correctly pointed out by one of the referees that it is sufficient for the solution of the inverse problem to invert  $\partial U / \partial |\mathbf{x}|$  instead of  $U$ . Furthermore, it has been correctly

pointed out that this latter inversion is much simpler since the expression for  $\partial U/\partial|\mathbf{x}|$  is simpler than the expression of  $U$  (see [5]).

(g) A short summary of the analytical results presented here was announced in [16].

### 2. Analytical results

We first show that equations (1.5) can be written in an alternative form, which is more convenient for determining the part of  $\mathbf{J}^p$  which can be reconstructed from the knowledge of  $U(\mathbf{x})$ .

**Theorem 1.** *Let  $U(\mathbf{x})$  be defined in terms of  $\mathbf{J}^p$  by equation (1.5). Then  $U(\mathbf{x})$  can also be expressed by the alternative representation*

$$U(\mathbf{x}) = -\frac{1}{4\pi} \int_{|\mathbf{y}| \leq 1} \frac{1}{|\mathbf{x} - \mathbf{y}|} \left( \frac{1}{|\mathbf{y}|^2} \int_{|\mathbf{z}| \leq 1} \{(\nabla_{\mathbf{z}} \wedge \mathbf{J}^p(\mathbf{z})) \cdot \mathbf{z}\}_{\mathbf{z}=\frac{|\mathbf{z}|}{|\mathbf{y}|}\mathbf{y}} |\mathbf{z}| d|\mathbf{z}| \right) d\mathbf{y}, \quad |\mathbf{x}| > 1. \tag{2.1}$$

**Proof.** Let  $I(\mathbf{z})$  denote the following function of  $\mathbf{z}$ ,

$$I(\mathbf{z}) = \frac{4\pi}{|\mathbf{z}|} \int_0^{|\mathbf{z}|} \{(\mathbf{J}^p(\mathbf{z}) \wedge \mathbf{x}) \cdot (\nabla_{\mathbf{x}} \Phi(\mathbf{x}))\}_{\mathbf{x}=\frac{|\mathbf{x}|}{|\mathbf{z}|}\mathbf{z}} d|\mathbf{x}|, \tag{2.2}$$

where  $\Phi(\mathbf{x}) \in C_0^\infty(\mathbb{R}^3)$ . We will integrate  $I(\mathbf{z})$  over the sphere  $|\mathbf{z}| \leq 1$ : we first multiply by  $|\mathbf{z}|^2$  and integrate with respect to  $d|\mathbf{z}|$  along  $0 < |\mathbf{z}| < 1$ . Interchanging in the resulting expression the order of the integration with respect to  $d|\mathbf{x}|$  and to  $d|\mathbf{z}|$  we find

$$\int_0^1 I(\mathbf{z}) |\mathbf{z}|^2 d|\mathbf{z}| = 4\pi \int_0^1 \{\nabla_{\mathbf{x}} \Phi(\mathbf{x})\}_{\mathbf{x}=\frac{|\mathbf{x}|}{|\mathbf{z}|}\mathbf{z}} \cdot \left( \int_{|\mathbf{z}|}^1 \mathbf{J}^p(\mathbf{z}) \wedge |\mathbf{x}| \mathbf{z} d|\mathbf{z}| \right) d|\mathbf{x}|.$$

We then integrate this equation with respect to  $d\hat{\mathbf{z}}$ ,  $\hat{\mathbf{z}} = \mathbf{z}/|\mathbf{z}|$ , and denote  $|\mathbf{x}| \hat{\mathbf{z}}$  by  $\mathbf{y}$ . This yields

$$\int_{|\mathbf{z}| \leq 1} I(\mathbf{z}) d\mathbf{z} = -4\pi \int_{|\mathbf{y}| \leq 1} \Phi(\mathbf{y}) \nabla_{\mathbf{y}} \cdot \left( \frac{1}{|\mathbf{y}|^2} \int_{|\mathbf{y}|}^1 \mathbf{J}^p \left( \frac{|\mathbf{z}|}{|\mathbf{y}|} \mathbf{y} \right) \wedge \mathbf{y} |\mathbf{z}| d|\mathbf{z}| \right) d\mathbf{y}. \tag{2.3}$$

It is straightforward to show that

$$\nabla_{\mathbf{y}} \cdot \left( \mathbf{J}^p \left( \frac{|\mathbf{z}|}{|\mathbf{y}|} \mathbf{y} \right) \wedge \mathbf{y} \right) = \frac{|\mathbf{z}|}{|\mathbf{y}|} \{ \nabla_{\mathbf{z}} \wedge \mathbf{J}^p(\mathbf{z}) \}_{\mathbf{z}=\frac{|\mathbf{z}|}{|\mathbf{y}|}\mathbf{y}} \cdot \mathbf{y}. \tag{2.4}$$

Indeed, the rhs of this equation equals

$$\frac{|\mathbf{z}|}{|\mathbf{y}|} \left( y_2 \frac{\partial J_1^p}{\partial z_3} - y_1 \frac{\partial J_2^p}{\partial z_3} \right) + cp, \tag{2.5}$$

where  $cp$  denotes cyclic permutation; the lhs of equation (2.4) equals

$$\frac{\partial}{\partial y_3} (y_2 J_1^p - y_1 J_2^p) + cp,$$

and using the chain rule as well as noting that several of the resulting terms cancel we find expression (2.5).

Using equation (2.4), as well as noting that the term  $\nabla_{\mathbf{y}}(|\mathbf{y}|^{-2})$  is perpendicular to  $\mathbf{J}^p \wedge \mathbf{y}$ , the rhs of equation (2.3) becomes

$$-4\pi \int_{|\mathbf{y}| \leq 1} \Phi(\mathbf{y}) \frac{1}{|\mathbf{y}|^2} \left( \int_{|\mathbf{y}|}^1 \{(\nabla_{\mathbf{z}} \wedge \mathbf{J}^p(\mathbf{z})) \cdot \mathbf{z}\}_{\mathbf{z}=\frac{|\mathbf{z}|}{|\mathbf{y}|}\mathbf{y}} |\mathbf{z}| d|\mathbf{z}| \right) d\mathbf{y}.$$

Replacing the rhs of equation (2.3) by this expression and replacing  $I(\mathbf{z})$  by the definition (2.2), equation (2.3) and the standard Green's function representation for solutions of

Poisson’s equation, give equation (2.1) provided that the result of the lemma proved in appendix A is valid. Note that according to our proof, equation (2.1) is valid in the distributional sense, but simple regularity arguments imply that it is also valid pointwise. QED

**Theorem 2 (representation theorem).** *The vector  $\mathbf{J}^p(\mathbf{x})$  can be uniquely decomposed in the form*

$$\mathbf{J}^p(\mathbf{x}) = J^\rho(\rho, \theta, \varphi)\mathbf{e}_\rho + J^\theta(\rho, \theta, \varphi)\mathbf{e}_\theta + J^\varphi(\rho, \theta, \varphi)\mathbf{e}_\varphi, \tag{2.6}$$

where  $\mathbf{e}_\rho, \mathbf{e}_\theta, \mathbf{e}_\varphi$  are the unit vectors associated with the spherical coordinates  $\rho > 0, 0 \leq \theta \leq \pi, 0 \leq \varphi < 2\pi$ , and the scalar functions  $J^\theta$  and  $J^\varphi$  can be represented in the form

$$J^\theta = \frac{1}{\rho} \left( \frac{\partial G}{\partial \theta} - \frac{1}{\sin \theta} \frac{\partial F}{\partial \varphi} \right), \quad J^\varphi = \frac{1}{\rho} \left( \frac{1}{\sin \theta} \frac{\partial G}{\partial \varphi} + \frac{\partial F}{\partial \theta} \right), \tag{2.7}$$

where  $G(\rho, \theta, \varphi)$  and  $F(\rho, \theta, \varphi)$  are scalar functions of the arguments included.

Assume that  $U(\mathbf{x})$  is defined in terms of  $\mathbf{J}^p$  by equation (1.5). Then

$$U(\mathbf{x}) = -\frac{1}{4\pi} \int_{|\mathbf{y}| \leq 1} \frac{1}{|\mathbf{x} - \mathbf{y}|} \left( \frac{1}{|\mathbf{y}|^2} \int_{|\mathbf{z}|}^1 \Delta_{\theta, \varphi} F(|\mathbf{z}|, \theta, \varphi) d|\mathbf{z}| \right) d\mathbf{y}, \quad |\mathbf{x}| > 1, \tag{2.8}$$

where  $\Delta_{\theta, \varphi}$  denotes the Laplacian with respect to the spherical coordinates  $\theta$  and  $\varphi$ , i.e.

$$\Delta_{\theta, \varphi} = \frac{1}{\sin \theta} \left[ \frac{\partial}{\partial \theta} \left( \sin \theta \frac{\partial}{\partial \theta} \right) + \frac{1}{\sin \theta} \frac{\partial^2}{\partial \varphi^2} \right].$$

**Proof.** We first decompose  $\mathbf{J}^p$  into a radial and a tangential component. Clearly  $J^\rho$  gives no contribution to  $U$ . Also the tangential component can be uniquely decomposed in the form (2.7), see appendix B. Using equations (2.6) and (2.7) we find

$$(\nabla \wedge \mathbf{J}^p) \cdot \mathbf{z} = \frac{1}{|\mathbf{z}|} \left( \frac{1}{\sin \theta} \frac{\partial}{\partial \theta} \sin \theta \frac{\partial F}{\partial \theta} + \frac{1}{\sin^2 \theta} \frac{\partial^2 F}{\partial \varphi^2} \right),$$

and (2.1) becomes equation (2.8). QED

**Corollary (non-uniqueness of the inverse problem).** *Assume that  $U(\mathbf{x})$  is defined in terms of  $\mathbf{J}^p$  by equation (1.5). Let the vector  $\mathbf{J}^p(\mathbf{x})$  be written in the form (2.6) where the scalar functions  $J^\theta$  and  $J^\varphi$  are given in terms of the scalar function  $G$  and  $F$  by equations (2.7).*

*The function  $U(\mathbf{x})$  is independent of  $J^\rho$  and of  $G$ , and furthermore only certain moments of  $F$  can be computed in terms of  $U$ . In particular,  $F(\rho, \theta, \varphi)$  is given by the expression*

$$F(\rho, \theta, \varphi) = \sum_{\ell=1}^{\infty} \sum_{m=-\ell}^{\ell} f_{\ell, m}(\rho) Y_{\ell, m}(\theta, \varphi), \quad \rho < 1, \quad 0 \leq \theta \leq \pi, \quad 0 \leq \varphi < 2\pi,$$

where  $Y_{\ell, m}$  are the usual spherical harmonics, the moments of  $f_{\ell, m}(\rho)$  can be determined in terms of  $c_{\ell, m}$ ,

$$\ell \int_0^1 \rho^{\ell+1} f_{\ell, m}(\rho) d\rho = (2\ell + 1)c_{\ell, m}, \tag{2.9}$$

and the constants  $c_{\ell, m}$  can be determined from the given data using the fact that  $U(\mathbf{x})$  can be expressed in the form

$$U(\rho, \theta, \varphi) = \sum_{\ell=1}^{\infty} \sum_{m=-\ell}^{\ell} c_{\ell, m} \rho^{-(\ell+1)} Y_{\ell, m}(\theta, \varphi), \quad \rho > 1, \quad 0 \leq \theta \leq \pi, \quad 0 \leq \varphi \leq 2\pi. \tag{2.10}$$

**Proof.** Equation (2.8) implies

$$\begin{aligned} \Delta U &= \frac{1}{|\mathbf{x}|^2} \int_{|\mathbf{z}|}^1 \Delta_{\theta, \varphi} F(|\mathbf{z}|, \theta, \varphi) d|\mathbf{z}|, & |\mathbf{x}| < 1, \\ \Delta U &= 0, & |\mathbf{x}| > 1. \end{aligned} \tag{2.11}$$

Let us represent  $F$  and  $U$  in terms of spherical harmonics by

$$F(\rho, \theta, \varphi) = \sum_{\ell, m} f_{\ell, m}(\rho) Y_{\ell, m}(\theta, \varphi) \quad \text{and} \quad U(\rho, \theta, \varphi) = \sum_{\ell, m} u_{\ell, m}(\rho) Y_{\ell, m}(\theta, \varphi).$$

Then equations (2.11) imply

$$u''_{\ell, m} + \frac{2}{\rho} u'_{\ell, m} - \frac{\ell(\ell + 1)}{\rho^2} u_{\ell, m} = \begin{cases} -\frac{\ell(\ell + 1)}{\rho^2} \int_{\rho}^1 f_{\ell, m}(\rho') d\rho' & \rho < 1 \\ 0 & \rho > 1, \end{cases}$$

where prime denotes differentiation with respect to  $\rho$ . The general solution of the homogeneous problem is  $\alpha\rho^\ell + \beta\rho^{-(\ell+1)}$ , where  $\alpha$  and  $\beta$  are constants and  $\ell$  is a positive integer. Since  $u_{\ell, m} \rightarrow 0$  as  $\rho \rightarrow \infty$  it follows that

$$u_{\ell, m} = c_{\ell, m} \rho^{-(\ell+1)}.$$

To solve the inhomogeneous problem, we use variation of parameters in the form  $u_{\ell, m}(\rho) = A_{\ell, m}(\rho)\rho^\ell$ . This implies

$$(A'_{\ell, m} \rho^{2\ell+2})' = -\ell(\ell + 1)\alpha_{\ell, m}(\rho), \quad \alpha_{\ell, m}(\rho) \doteq \rho^\ell \int_{\rho}^1 f_{\ell, m}(\rho') d\rho'.$$

Thus,

$$A'_{\ell, m} \rho^{2\ell+2} = \ell(\ell + 1) \int_{\rho}^1 \alpha_{\ell, m}(\rho') d\rho' + A'_{\ell, m}(1).$$

Convergence at  $\rho = 0$  implies

$$A'_{\ell, m}(1) + \ell(\ell + 1) \int_0^1 \alpha_{\ell, m}(\rho') d\rho' = 0. \tag{2.12}$$

Using  $A_{\ell, m} = u_{\ell, m} \rho^{-\ell}$ , we find

$$A'_{\ell, m}(1) = u'_{\ell, m}(1) - \ell u_{\ell, m}(1) = (c_{\ell, m} \rho^{-(\ell+1)})'|_{\rho=1} - \ell c_{\ell, m} \rho^{-(\ell+1)}|_{\rho=1} = -(2\ell + 1)c_{\ell, m}.$$

This equation together with (2.12) implies

$$\ell(\ell + 1) \int_0^1 \alpha_{\ell, m}(\rho) d\rho = (2\ell + 1)c_{\ell, m}.$$

Using integration by parts we find (2.9). QED

**Theorem 3 (minimization of energy).** Define the energy by

$$W \doteq \int_{|\mathbf{x}| \leq 1} |\mathbf{J}^p|^2 d\mathbf{x}. \tag{2.13}$$

Then if

$$\mathbf{J}^p = J^\rho \mathbf{e}_\rho + J^\theta \mathbf{e}_\theta + J^\varphi \mathbf{e}_\varphi,$$

where  $J^\theta$  and  $J^\varphi$  are given by equations (2.7), it follows that the minimum of  $W$  under the constrain

$$F = \sum_{\ell=1}^{\infty} \sum_{m=-\ell}^{\ell} f_{\ell, m}(\rho) Y_{\ell, m}(\theta, \varphi), \quad \ell \int_0^1 \rho^{\ell+1} f_{\ell, m}(\rho) d\rho = (2\ell + 1)c_{\ell, m},$$

where  $Y_{\ell,m}$  are the usual spherical harmonics and  $c_{\ell,m}$  are given constants, is achieved when

$$J^\rho = G = 0, \quad F = \sum_{\ell=1}^{\infty} \sum_{m=-\ell}^{\ell} \frac{(2\ell+1)(2\ell+3)}{\ell} c_{\ell,m} \rho^{\ell+1} Y_{\ell,m}(\theta, \varphi). \tag{2.14}$$

**Proof.** Substituting equations (2.6) and (2.7) in the rhs of equation (2.13) we find

$$W = \int_{|\mathbf{x}| \leq 1} \left[ (J^\rho)^2 + \frac{1}{\rho^2} \left( \frac{\partial G}{\partial \theta} \right)^2 + \frac{1}{\rho^2 \sin^2 \theta} \left( \frac{\partial G}{\partial \varphi} \right)^2 + \frac{1}{\rho^2 \sin^2 \theta} \left( \frac{\partial F}{\partial \varphi} \right)^2 + \frac{1}{\rho^2} \left( \frac{\partial F}{\partial \theta} \right)^2 \right] d\mathbf{x},$$

where we have used that the term involving  $G_\varphi F_\theta - G_\theta F_\varphi$  vanishes,

$$\int_0^1 \int_0^\pi \int_0^{2\pi} \frac{1}{\rho^2 \sin \theta} \left[ -\frac{\partial G}{\partial \theta} \frac{\partial F}{\partial \varphi} + \frac{\partial G}{\partial \varphi} \frac{\partial F}{\partial \theta} \right] \rho^2 \sin \theta \, d\rho \, d\theta \, d\varphi = 0.$$

The constraint involves only  $F$ , thus it follows that the minimal energy is achieved when  $J^\rho = G = 0$  and when  $H$  is minimal, where

$$H = \int_0^1 \int_0^\pi \int_0^{2\pi} \left[ \frac{1}{\rho^2 \sin^2 \theta} \left( \frac{\partial F}{\partial \varphi} \right)^2 + \frac{1}{\rho^2} \left( \frac{\partial F}{\partial \theta} \right)^2 \right] \rho^2 \sin \theta \, d\rho \, d\theta \, d\varphi. \tag{2.15}$$

The term inside the bracket equals  $|\nabla F|^2 - \left( \frac{\partial F}{\partial \rho} \right)^2$ , which using integration by parts (with either  $F$  or  $\frac{\partial F}{\partial \rho}$  equal to 0 at  $|\mathbf{x}| = 1$ ) equals  $-[F \Delta F + \left( \frac{\partial F}{\partial \rho} \right)^2]$ , where

$$\Delta F = \frac{\partial^2 F}{\partial \rho^2} + \frac{2}{\rho} \frac{\partial F}{\partial \rho} + \frac{1}{\rho^2} \Delta_{\theta,\varphi} F.$$

Using

$$F = \sum_{\ell,m} f_{\ell,m}(\rho) Y_{\ell,m}(\theta, \varphi), \quad \Delta_{\theta,\varphi} Y_{\ell,m} = -\ell(\ell+1) Y_{\ell,m},$$

and the orthogonality of the spherical harmonics, it follows that

$$H = - \sum_{\ell,m} \int_0^1 \left\{ \left[ f_{\ell,m}''(\rho) + \frac{2}{\rho} f_{\ell,m}'(\rho) - \frac{\ell(\ell+1)}{\rho^2} f_{\ell,m}(\rho) \right] f_{\ell,m}(\rho) + (f_{\ell,m}'(\rho))^2 \right\} \rho^2 \, d\rho.$$

Hence,

$$H = - \sum_{\ell,m} \left[ \int_0^1 \{ (f_{\ell,m} f_{\ell,m}' \rho^2)' - \ell(\ell+1) f_{\ell,m}^2(\rho) \} \, d\rho \right].$$

Thus, provided that either  $f_{\ell,m}(1)$  or  $f_{\ell,m}'(1)$  equals zero<sup>4</sup>, we find

$$H = \sum_{\ell,m} \ell(\ell+1) \int_0^1 f_{\ell,m}^2(\rho) \, d\rho.$$

The assumption that  $f_{\ell,m}(1) = 0$  is without loss of generality since the tangential part of the energy which is given by equation (2.15) does not involve differentiation over  $\rho$ , thus in general (2.15) can be obtained by approximating  $f$  by functions equal to zero at  $\rho = 1$  and then passing to the limit.

The minimization of this  $H$ , under the constraint (2.9), implies (2.14).

We note that equation (1.5) implies that  $U(\mathbf{x})$  behaves like  $0(\rho^{-2})$ , hence  $\ell > 0$  in equation (2.10),  $c_{00} = 0$ , and the sum (2.14) starts with  $\ell = 1$ . QED

<sup>4</sup> These conditions are true since the support of  $\mathbf{J}^p$  lies in the interior of the sphere.

### 3. Numerical implementation

In equation (2.10),  $Y_{\ell,m}$  denotes the spherical harmonics, namely

$$\begin{aligned} Y_{\ell,m}(\theta, \varphi) &= a_{\ell,m} P_{\ell,m}(\cos \theta) e^{im\varphi}, \\ Y_{\ell,-m} &= (-1)^m \overline{Y_{\ell,m}}, \quad \ell \geq 1, \quad 0 \leq m \leq \ell, \end{aligned} \tag{3.1}$$

where the bar denotes complex conjugate and

$$a_{\ell,m} = \sqrt{\frac{2\ell + 1}{4\pi} \frac{(\ell - m)!}{(\ell + m)!}}. \tag{3.2}$$

$P_{\ell,m}$  are the Legendre functions, namely

$$P_{\ell,m}(x) = (-1)^m (1 - x^2)^{m/2} \frac{d^m}{dx^m} P_{\ell}(x),$$

where

$$P_{\ell}(x) = \frac{1}{2^{\ell} \ell!} \frac{d^{\ell}}{dx^{\ell}} (x^2 - 1)^{\ell}$$

are the usual Legendre polynomials of degree  $\ell$ .

For the numerical implementation, we replace in the sums appearing in (2.10), (2.14),  $\infty$  by  $\ell_{\max}$ , where  $\ell_{\max}$  is chosen by the procedure explained below.

#### 3.1. Computation of $c_{\ell,m}$

We first discuss how to compute  $c_{\ell,m}$  from either  $U(\rho, \theta, \varphi)$  or  $\mathbf{B}(\rho, \theta, \varphi)$ . Suppose we know  $U(\rho, \theta, \varphi)$  for one specific value of  $\rho > 1$  and for some equally spaced values  $\theta_i, \varphi_j$ , such as

$$\begin{aligned} 0 \leq \theta_i \leq \pi, & \quad i = 0, \dots, i_{\max}, \\ 0 \leq \varphi_j < 2\pi, & \quad j = 0, \dots, j_{\max}. \end{aligned}$$

Using the orthogonality of  $Y_{\ell,m}$  equation (2.10) implies

$$\int_0^{2\pi} \left( \int_{-1}^1 U(\theta, \varphi) \overline{Y_{\ell,m}(\theta, \varphi)} d(\cos \theta) \right) d\varphi = c_{\ell,m} \rho^{-(\ell+1)}.$$

Therefore, using the first equation in (3.1), we obtain

$$c_{\ell,m} = \rho^{\ell+1} a_{\ell,m} \int_0^{2\pi} \left( \int_0^{\pi} U(\theta, \varphi) P_{\ell,m}(\cos \theta) \sin \theta d\theta \right) e^{-im\varphi} d\varphi.$$

Using (3.1), we find

$$\begin{aligned} c_{\ell,m} &= \rho^{\ell+1} a_{\ell,m} \hat{U}_{\ell,m}, \\ c_{\ell,-m} &= (-1)^m \overline{c_{\ell,m}}, \quad \ell \geq 1, \quad 0 \leq m \leq \ell, \end{aligned} \tag{3.3}$$

where

$$\hat{U}_{\ell,m} = \int_0^{2\pi} \tilde{U}_{\ell,m}(\varphi) \cos m\varphi d\varphi - i \int_0^{2\pi} \tilde{U}_{\ell,m}(\varphi) \sin m\varphi d\varphi, \tag{3.4}$$

and

$$\tilde{U}_{\ell,m}(\varphi) = \int_0^{\pi} U(\theta, \varphi) P_{\ell,m}(\cos \theta) \sin \theta d\theta. \tag{3.5}$$

For the numerical calculation of the three integrals appearing in (3.4) and (3.5), we use an extended closed formula, namely,

$$\int_{x_1}^{x_n} f(x) dx = \Delta x \left( \frac{3}{8} f_1 + \frac{7}{6} f_2 + \frac{23}{24} f_3 + f_4 + \cdots + f_{n-3} + \frac{23}{24} f_{n-2} + \frac{7}{6} f_{n-1} + \frac{3}{8} f_n \right).$$

For the numerical calculation of the Legendre functions  $P_{\ell,m}(\cos \theta)$ , we use the subroutine `plgndr` from *Numerical Recipes* [17]. The constants  $a_{\ell,m}$  are given by (3.2).

Suppose we know  $\mathbf{B} = (B_1, B_2, B_3)$  instead of  $U$ . Then, using the first relation in (1.5) and spherical coordinates we obtain

$$U_\rho = \sin \theta \cos \varphi \tilde{B}_1 + \sin \theta \sin \varphi \tilde{B}_2 + \cos \theta \tilde{B}_3, \quad (3.6)$$

where

$$\tilde{B}_i = \frac{B_i(\rho, \theta, \varphi)}{\mu_0}, \quad i = 1, 2, 3.$$

Moreover, by differentiating (2.10) with respect to  $\rho$  we find

$$U_\rho(\rho, \theta, \varphi) = - \sum_{\ell=1}^{\ell_{\max}} \sum_{m=-\ell}^{\ell} c_{\ell,m}(\ell+1)\rho^{-(\ell+2)} Y_{\ell,m}(\theta, \varphi). \quad (3.7)$$

Thus, if we know  $\mathbf{B}$ , we can compute  $U_\rho$  from (3.6) and then we can compute  $c_{\ell,m}$  from (3.7), following the same procedure as before.

*The choice of  $\ell_{\max}$ .* Using (3.1) and the second relation in (3.3), the real part of (2.10) implies

$$U(\rho, \theta, \varphi) = \sum_{\ell=1}^{\ell_{\max}} \rho^{-(\ell+1)} \left( \operatorname{Re}(c_{\ell,0}) a_{\ell,0} P_{\ell,0}(\cos \theta) + 2 \sum_{m=1}^{\ell} (\operatorname{Re}(c_{\ell,m}) \cos m\varphi - \operatorname{Im}(c_{\ell,m}) \sin m\varphi) a_{\ell,m} P_{\ell,m}(\cos \theta) \right). \quad (3.8)$$

Differentiation with respect to  $\rho$  yields

$$U_\rho(\rho, \theta, \varphi) = - \sum_{\ell=1}^{\ell_{\max}} (\ell+1)\rho^{-(\ell+2)} \left( \operatorname{Re}(c_{\ell,0}) a_{\ell,0} P_{\ell,0}(\cos \theta) + 2 \sum_{m=1}^{\ell} (\operatorname{Re}(c_{\ell,m}) \cos m\varphi - \operatorname{Im}(c_{\ell,m}) \sin m\varphi) a_{\ell,m} P_{\ell,m}(\cos \theta) \right). \quad (3.9)$$

Therefore, after calculating the coefficients  $c_{\ell,m}$  following the procedure outlined earlier we can use either (3.8) or (3.9) to re-evaluate either  $U$  or  $U_\rho$ . In this way not only can we test the efficiency of our procedure, but we can also run our program several times, in order to find the most appropriate value for  $\ell_{\max}$ .

### 3.2. Computation of the minimizing current

Using relations (2.14), (3.1) and the second relation in (3.3), the real parts of the functions  $J^\theta$ ,  $J^\varphi$  defined in (2.7) (with  $G = 0$ ) are given by

$$J^\theta(\rho, \theta, \varphi) = \frac{2}{\sin \theta} \sum_{\ell=1}^{\ell_{\max}} \frac{(2\ell+1)(2\ell+3)}{\ell} \rho^\ell \left( \sum_{m=1}^{\ell} m (\operatorname{Re}(c_{\ell,m}) \sin m\varphi + \operatorname{Im}(c_{\ell,m}) \cos m\varphi) a_{\ell,m} P_{\ell,m}(\cos \theta) \right), \quad (3.10)$$

and

$$\begin{aligned}
 J^\varphi(\rho, \theta, \varphi) = & -\sin \theta \sum_{\ell=1}^{\ell_{\max}} \frac{(2\ell+1)(2\ell+3)}{\ell} \rho^\ell \left( \operatorname{Re}(c_{\ell,0}) a_{\ell,0} P'_{\ell,0}(\cos \theta) \right. \\
 & \left. + 2 \sum_{m=1}^{\ell} (\operatorname{Re}(c_{\ell,m}) \cos m\varphi - \operatorname{Im}(c_{\ell,m}) \sin m\varphi) a_{\ell,m} P'_{\ell,m}(\cos \theta) \right). \tag{3.11}
 \end{aligned}$$

Recall that the Legendre functions satisfy the recurrence relation

$$P'_{\ell,m}(x) = -\frac{mx}{1-x^2} P_{\ell,m}(x) - \frac{1}{\sqrt{1-x^2}} P_{\ell,m+1}(x).$$

Therefore,

$$\begin{aligned}
 -\sin \theta P'_{\ell,0}(\cos \theta) &= P_{\ell,1}(\cos \theta), & \text{for } m = 0, \\
 -\sin \theta P'_{\ell,m}(\cos \theta) &= \frac{m \cos \theta}{\sin \theta} P_{\ell,m}(\cos \theta) + P_{\ell,m+1}(\cos \theta), & \text{for } m > 0.
 \end{aligned} \tag{3.12}$$

Thus, in order to calculate numerically the current we apply the following procedure: we take some  $\theta$  and  $\varphi$  points, such that  $0 \leq \theta \leq \pi$ ,  $0 \leq \varphi \leq 2\pi$ . We first calculate the Legendre functions  $P_{\ell,m}(\cos \theta)$ . In a separate subroutine, we calculate the quantities  $P_{\ell,m}(\cos \theta)/\sin \theta$  (for this purpose, we have developed a subroutine similar to `p1gndr`). These quantities appear in both (3.10) and in the second relation of (3.12). Note that these quantities are valid even for  $\theta = 0$  or  $\theta = \pi$ . We then calculate from (3.12) the quantities  $-\sin \theta P'_{\ell,m}(\cos \theta)$ . Finally, we take a value of  $\rho$  such as  $0 < \rho < 1$  and calculate  $J^\theta(\rho, \theta, \varphi)$  from (3.10) and  $J^\varphi(\rho, \theta, \varphi)$  from (3.11). In all the above calculations we use the  $\ell_{\max}$  value that was found with the procedure outlined in the previous subsection.

### 3.3. Verification of the algorithm

We have tested our numerical algorithm for several functions  $U(\rho, \theta, \varphi)$ . In what follows we discuss two typical examples.

**Example 1.** Let  $U$  be given by

$$U(\rho, \theta, \varphi) = -2 \cos \theta \frac{1}{\rho^2} + \sin \theta \cos \theta \cos \varphi \frac{1}{\rho^3} - \sin^2 \theta \cos 2\varphi \frac{1}{\rho^3}.$$

Note that this function has the form (2.10) with  $c_{\ell,m} = 0$  for  $\ell > 2$ .

First, we evaluate  $U$  for  $\rho = 1.5$  and some equally spaced  $\theta_i$  and  $\varphi_j$ , where  $i_{\max} = 100, j_{\max} = 200$ . We calculate numerically the coefficients  $c_{\ell,m}$  using the first relation of (3.3), as well as (3.4) and (3.5). We then evaluate  $U_a$ , the approximate value of  $U$ , at the above  $\rho, \theta_i$  and  $\varphi_j$  using (3.8). Furthermore, we start with  $U_\rho$  instead of  $U$ ; we calculate  $c_{\ell,m}$  in a similar way and then calculate the approximate value of  $U_\rho$  using (3.9).

We run our program several times with  $l_{\max}$  from 1 to 40 and found that the best value is  $l_{\max} = 2$ , which is consistent with the exact form of  $U$ . For this value, the difference  $|U - U_a|$  is of the order of  $10^{-7}$ , at most.

Secondly, we calculate numerically  $J^\theta, J^\varphi$ , using (3.10)–(3.12), in the above  $\theta_i, \varphi_j$  and some equally spaced  $\rho_k$ , such as  $0 \leq \rho_k \leq 1$ , namely  $k = 0, \dots, k_{\max}$ , where  $k_{\max} = 25$ . Then we calculate *analytically*  $c_{\ell,m}$  using (2.10),  $F$  using (2.14), and  $J_\theta, J_\varphi$  using (2.7). For the above  $U$ , we have

$$F = -30\rho^2 \sin \theta + \frac{35}{2}\rho^3 \sin \theta \cos \theta \cos \varphi - \frac{35}{2}\rho^3 \sin^2 \theta \cos 2\varphi. \tag{3.13}$$

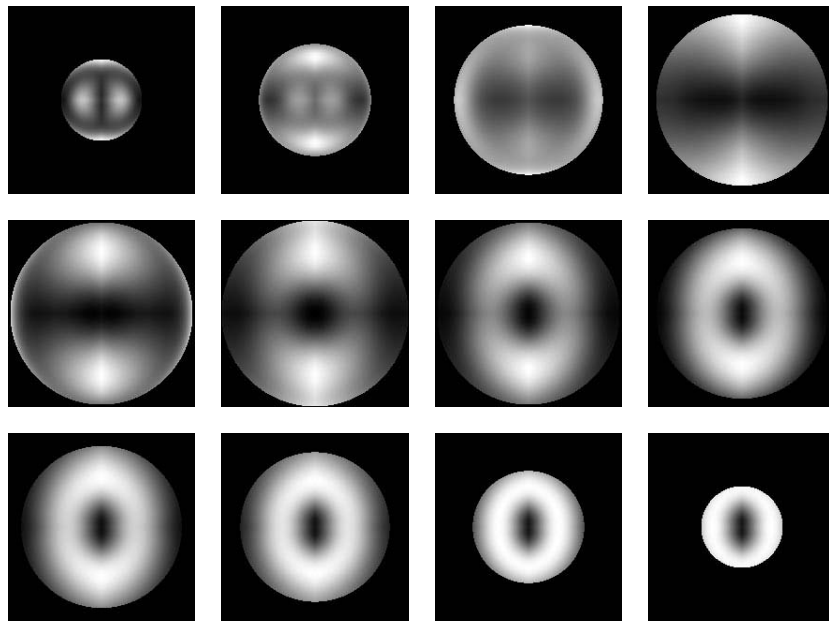


**Figure 1.** Density plots for the minimizing current of the function  $U$  given by (3.14). Starting from top left  $x_3 = -0.9, -0.8, -0.6, -0.4, -0.2, 0, 0.2, 0.4, 0.5, 0.6, 0.8$  and  $0.9$ .

The analytical and the numerical values of  $J^\theta$  and  $J^\varphi$  in the various  $\theta_i, \varphi_j$  and  $\rho_k$  are almost the same (the absolute value of their difference is of the order of  $10^{-7}$ , at most).

We have also verified the validity of equation (2.8) as follows: we compute  $F$  using (3.13) and evaluate numerically  $U_a$  using (2.8);  $|U - U_a|$  is of the order of  $10^{-5}$ , at most.

**Example 2.** Let  $U$  be given by

$$U = \frac{1}{4\pi} \frac{p_1 x_1 + p_2 x_2 + p_3 (x_3 - a)}{[x_1^2 + x_2^2 + (x_3 - a)^2]^{3/2}} \tag{3.14}$$

with  $a = 0.5$  and  $(p_1, p_2, p_3) = (0.1, -0.2, 0.6)$ . We evaluate  $U$  for  $\rho = 1.5$  and for the same equally spaced  $\theta_i$  and  $\varphi_j$ , as in example 1. We again calculate numerically the coefficients  $c_{\ell,m}$  and then  $U_a$ .

For this example we found that the best value for  $l_{\max}$  is 10. For this value the difference  $|U - U_a|$  is of the order of  $10^{-6}$ , at most.

In figure 1, we present the density plots of the minimizing current  $(J^\theta)^2 + (J^\varphi)^2$  for the above function  $U$  in various cuts perpendicular to the  $x_3$ -axis.

**Acknowledgments**

This is part of a project jointly undertaken by the authors, A A Ioannides and I M Gel'fand. ASF is grateful to A A Ioannides for introducing him to MEG and for numerous important discussions. This research was partially supported by the EPSRC. VM was supported by a Marie Curie Individual Fellowship of the European Community under contract number HPMF-CT-2002-01597. We are grateful to the two referees for several important remarks.

**Appendix A**

**Lemma.** *Let*

$$U(\mathbf{x}, \mathbf{z}) \doteq \left( \frac{\mathbf{J}(\mathbf{z}) \wedge \mathbf{z}}{|\mathbf{x} - \mathbf{z}|(|\mathbf{x}||\mathbf{x} - \mathbf{z}| + \mathbf{x} \cdot (\mathbf{x} - \mathbf{z}))} \right) \cdot \mathbf{x}. \tag{A.1}$$

*Then*

$$\int_{\mathbb{R}^3} (\Delta_{\mathbf{x}} U(\mathbf{x}, \mathbf{z})) \Phi(\mathbf{x}) \, d\mathbf{x} = -\frac{4\pi}{|\mathbf{z}|} \int_0^{|\mathbf{z}|} \{(\mathbf{J}(\mathbf{z}) \wedge \mathbf{x}) \cdot (\nabla_{\mathbf{x}} \Phi(\mathbf{x}))\}_{\mathbf{x}=|\mathbf{x}'|\frac{\mathbf{z}}{|\mathbf{z}|}} \, d|\mathbf{x}'|, \tag{A.2}$$

where  $\Delta$  is the Laplacian (i.e.  $\Delta = \nabla \cdot \nabla$ ) and  $\Phi(\mathbf{x}) \in C_0^\infty(\mathbb{R}^3)$ .

**Remark.** As  $\Delta U$  is singular close to  $\mathbf{x} = |\mathbf{x}'|\frac{\mathbf{z}}{|\mathbf{z}|}$ , the integral on the lhs of (A.2) should be understood in the sense of distributions.

**Proof.** Let  $\mathbf{z}$  be at distance  $a$  from the origin along the direction  $x'_3$ . Let  $\Omega_\epsilon(\mathbf{z})$  denote a small neighbourhood of the interval  $[0, \mathbf{z}]$  defined as follows:

$$\Omega_\epsilon(\mathbf{z}) = C_\epsilon(\mathbf{z}) \cup S_\epsilon(0) \cup S_\epsilon(\mathbf{z}),$$

where  $C_\epsilon(\mathbf{z})$  is the cylindrical region

$$C_\epsilon(\mathbf{z}) = \{\mathbf{x}' \in \mathbb{R}^3: \rho = \sqrt{x_1'^2 + x_2'^2} = \epsilon, 0 \leq x_3' \leq a\},$$

while  $S_\epsilon(0)$  and  $S_\epsilon(\mathbf{z})$  are the semi-spherical regions

$$S_\epsilon(0) = \{\mathbf{x}' \in \mathbb{R}^3: |\mathbf{x}'| = \epsilon, x_3' < 0\},$$

and

$$S_\epsilon(\mathbf{z}) = \{\mathbf{x}' \in \mathbb{R}^3: |\mathbf{x}' - \mathbf{z}| = \epsilon, x_3' > a\},$$

respectively.

Let  $\Phi(\mathbf{x})$  be a test function, then from the theory of distributions it follows that

$$\begin{aligned} \Delta U(\Phi) &= \int_{\mathbb{R}^3} (\Delta U(\mathbf{x}, \mathbf{z})) \Phi(\mathbf{x}) \, d\mathbf{x} \doteq \int_{\mathbb{R}^3} U(\mathbf{x}, \mathbf{z}) \Delta \Phi(\mathbf{x}) \, d\mathbf{x} \\ &= \lim_{\epsilon \rightarrow 0} \int_{\mathbb{R}^3 / \Omega_\epsilon(\mathbf{z})} U(\mathbf{x}, \mathbf{z}) \Delta \Phi(\mathbf{x}) \, d\mathbf{x} = -\lim_{\epsilon \rightarrow 0} \int_{\partial \Omega_\epsilon(\mathbf{z})} \left( U \frac{\partial \Phi}{\partial n} - \frac{\partial U}{\partial n} \Phi \right) \, dS, \end{aligned} \tag{A.3}$$

where  $dS$  denotes the infinitesimal surface element on the surface  $\partial \Omega_\epsilon(\mathbf{z})$ ,  $n$  denotes the unit outward normal, and we have used the fact that  $\Delta U = 0$  in  $\mathbb{R}^3 / \Omega_\epsilon(\mathbf{z})$ . Let  $I_1(\mathbf{z}, \epsilon)$ ,  $I_2(\mathbf{z}, \epsilon)$ ,  $I_3(\mathbf{z}, \epsilon)$  denote the contributions from the integration along  $C_\epsilon(\mathbf{z})$ ,  $S_\epsilon(0)$  and  $S_\epsilon(\mathbf{z})$ , respectively. It is easy to show that  $\lim_{\epsilon \rightarrow 0} I_2 = \lim_{\epsilon \rightarrow 0} I_3 = 0$ . We now compute  $I_1$ : let

$$f(\mathbf{x}', \mathbf{z}) \doteq |\mathbf{x}' - \mathbf{z}|(|\mathbf{x}'||\mathbf{x}' - \mathbf{z}| + \mathbf{x}' \cdot (\mathbf{x}' - \mathbf{z})).$$

Thus, if  $\mathbf{x}' \in C_\epsilon(\mathbf{z})$ ,

$$f = [(a - x_3')^2 + \rho^2] \sqrt{\rho^2 + x_3'^2} + \sqrt{\rho^2 + (a - x_3')^2} (\rho^2 + x_3'^2 - ax_3').$$

Hence,

$$\begin{aligned} \frac{\partial f}{\partial \rho} &= 2\rho \sqrt{\rho^2 + x_3'^2} + \frac{\rho}{\sqrt{\rho^2 + x_3'^2}} [\rho^2 + (a - x_3')^2] \\ &\quad + 2\rho \sqrt{\rho^2 + (a - x_3')^2} + \frac{\rho(\rho^2 + x_3'^2 - ax_3')}{\sqrt{\rho^2 + (a - x_3')^2}}, \end{aligned}$$

and

$$\frac{\partial^2 f}{\partial \rho^2} = 2\sqrt{\rho^2 + x_3'^2} + \frac{\rho^2 + (a - x_3')^2}{\sqrt{\rho^2 + x_3'^2}} + 2\sqrt{\rho^2 + (a - x_3')^2} + \frac{\rho^2 + x_3'^2 - ax_3'}{\sqrt{\rho^2 + (a - x_3')^2}} + \rho \tilde{f},$$

where  $\tilde{f}$  is bounded at  $\rho = 0$ . Evaluating  $f$ ,  $\frac{\partial f}{\partial \rho}$  and  $\frac{\partial^2 f}{\partial \rho^2}$  at  $\rho = 0$ , we find

$$\begin{aligned} f|_{\rho=0} &= x_3'(a - x_3')^2 + (a - x_3')(x_3'^2 - ax_3') = 0, \\ \frac{\partial f}{\partial \rho} \Big|_{\rho=0} &= 0, \\ \frac{\partial^2 f}{\partial \rho^2} \Big|_{\rho=0} &= 2x_3' + \frac{(a - x_3')^2}{x_3'} + 2(a - x_3') + \frac{x_3'^2 - ax_3'}{a - x_3'} = \frac{a^2}{x_3'}. \end{aligned} \tag{A.4}$$

The integral (A.3) involves  $-U \frac{\partial \Phi}{\partial \rho} + \Phi \frac{\partial U}{\partial \rho}$ . Also, since

$$\mathbf{x}' = (x_1', x_2', x_3'), \quad \mathbf{z} = (0, 0, a), \quad \mathbf{J} = (J_1, J_2, J_3),$$

it follows that

$$(\mathbf{J}(\mathbf{z}) \wedge \mathbf{z}) \cdot \mathbf{x}' = a(J_2 x_1' - x_2' J_1) = a\rho(J_2 \cos \varphi' - J_1 \sin \varphi'),$$

where we have used  $x_1' = \rho \cos \varphi'$  and  $x_2' = \rho \sin \varphi'$ .

Equations (A.1) and (A.3) imply that we need to compute

$$\lim_{\rho \rightarrow 0} \int_0^{2\pi} \int_0^{|z|=a} \rho \, d\varphi' dx_3' [a(J_2 \cos \varphi' - J_1 \sin \varphi')] \left\{ -\frac{\rho}{f} \frac{\partial \Phi}{\partial \rho} + \Phi \left( \frac{1}{f} - \frac{\rho}{f^2} \frac{\partial f}{\partial \rho} \right) \right\}. \tag{A.5}$$

However,  $\Phi(\mathbf{x}') = \Phi(\rho \cos \varphi', \rho \sin \varphi', x_3')$ , thus as  $\rho \rightarrow 0$ ,

$$\Phi = \Phi(0, 0, x_3') + \rho \cos \varphi' \frac{\partial \Phi}{\partial x_1'}(0, 0, x_3') + \rho \sin \varphi' \frac{\partial \Phi}{\partial x_2'}(0, 0, x_3') + o(\rho^2),$$

and

$$\frac{\partial \Phi}{\partial \rho} = \cos \varphi' \frac{\partial \Phi}{\partial x_1'}(0, 0, x_3') + \sin \varphi' \frac{\partial \Phi}{\partial x_2'}(0, 0, x_3') + o(\rho).$$

Substituting the expressions for  $\Phi$  and for  $\frac{\partial \Phi}{\partial \rho}$  in (A.5), it follows that the rhs of equation (A.3) involves

$$\lim_{\rho \rightarrow 0} \int_0^{2\pi} \frac{a\rho^3}{f^2} \frac{\partial f}{\partial \rho} \left( J_1 \sin^2 \varphi' \frac{\partial \Phi}{\partial x_2'} - J_2 \cos^2 \varphi' \frac{\partial \Phi}{\partial x_1'} \right) d\varphi' = a\pi \left( J_1 \frac{\partial \Phi}{\partial x_2'} - J_2 \frac{\partial \Phi}{\partial x_1'} \right) \lim_{\rho \rightarrow 0} \frac{\rho^3}{f^2} \frac{\partial f}{\partial \rho}.$$

But

$$\lim_{\rho \rightarrow 0} \frac{\rho}{f} \frac{\partial f}{\partial \rho} = \lim_{\rho \rightarrow 0} \frac{\frac{\partial f}{\partial \rho} + \rho \frac{\partial^2 f}{\partial \rho^2}}{\frac{\partial f}{\partial \rho}} = 1 + \lim_{\rho \rightarrow 0} \frac{\frac{\partial^2 f}{\partial \rho^2} + \rho \frac{\partial^3 f}{\partial \rho^3}}{\frac{\partial^2 f}{\partial \rho^2}} = 2.$$

Also

$$\lim_{\rho \rightarrow 0} \frac{\rho^2}{f} = \lim_{\rho \rightarrow 0} \frac{2}{f_{\rho\rho}} = \frac{2x_3'}{a^2}.$$

Thus,

$$\lim_{\rho \rightarrow 0} \frac{\rho^3}{f^2} \frac{\partial f}{\partial \rho} = 4 \lim_{\rho \rightarrow 0} \frac{1}{f_{\rho\rho}} = 4 \frac{x_3'}{a^2},$$

where we have used (A.4). Hence,

$$\lim_{\epsilon \rightarrow 0} I_1 = \frac{4\pi}{a} \int_0^a \left[ J_1(\mathbf{z}) \frac{\partial \Phi}{\partial x_2'}(0, 0, x_3') - J_2(\mathbf{z}) \frac{\partial \Phi}{\partial x_1'}(0, 0, x_3') \right] x_3' \, dx_3'.$$

In the above derivation, we have used the convenient set of coordinates  $\mathbf{x}'$ , such that  $\mathbf{z}$  is along  $x_3'$ . This result can be immediately generalized by writing  $I_1$  in an invariant form. Then (A.2) follows.  $\square$

## Appendix B

We will show that  $J^\theta$  and  $J^\varphi$  can be expressed by equation (2.7). Indeed, if

$$\mathbf{J} = J^\theta \mathbf{e}_\theta + J^\varphi \mathbf{e}_\varphi,$$

then the corresponding 1-form on the sphere of radius  $\rho$  is

$$\alpha^\theta d\theta + \alpha^\varphi d\varphi, \quad J^\theta = \frac{1}{\rho} \alpha^\theta, \quad J^\varphi = \frac{1}{\rho \sin \theta} \alpha^\varphi.$$

On a compact Riemannian manifold, any 1-form  $\alpha$  has the unique decomposition

$$\alpha = dG + (-1) *d*\beta + \alpha^h,$$

where  $G$  is a function,  $\beta$  is a 2-form,  $\alpha^h$  is a harmonic 1-form and  $*$  is the Hodge operator. Also there do not exist any nonzero harmonic 1-forms on the sphere. Furthermore,  $*\beta = F$ , where  $F$  is a function. Hence,

$$\alpha = dG + (-1) *dF.$$

Using

$$dG = \frac{\partial G}{\partial \theta} d\theta + \frac{\partial G}{\partial \varphi} d\varphi,$$

and

$$*dF = \frac{1}{\sin \theta} \frac{\partial F}{\partial \varphi} d\theta - \sin \theta \frac{\partial F}{\partial \theta} d\varphi,$$

we find

$$\alpha^\theta = \frac{\partial G}{\partial \theta} - \frac{1}{\sin \theta} \frac{\partial F}{\partial \varphi}, \quad \alpha^\varphi = \frac{\partial G}{\partial \varphi} + \sin \theta \frac{\partial F}{\partial \theta},$$

and equations (2.7) follow.

**Remark.** In the case of  $\mathbb{R}^3$ , the analogous decomposition is given by Helmholtz theorem: let  $\mathbf{A} = A^x \mathbf{i} + A^y \mathbf{j} + A^z \mathbf{k}$ , where  $\mathbf{i}, \mathbf{j}, \mathbf{k}$  are the unit vectors along the  $x$ -,  $y$ -,  $z$ -axis, be a vector field in  $\mathbb{R}^3$ . Then there exists a function  $G$  and a vector field  $\mathbf{B} = B^x \mathbf{i} + B^y \mathbf{j} + B^z \mathbf{k}$  such that  $\mathbf{A} = \nabla G + \nabla \wedge \mathbf{B}$ . A relationship between the general decomposition and the one in  $\mathbb{R}^3$  can be established using the following facts: (i) a differential 1-form  $\alpha = \alpha^x dx + \alpha^y dy + \alpha^z dz$  can be canonically identified with the vector field  $\mathbf{A}$ , where  $A^x = \alpha^x$ ,  $A^y = \alpha^y$ ,  $A^z = \alpha^z$ . (ii) In  $\mathbb{R}^3$  the Hodge operator transforms a differential 1-form  $\alpha$  into the differential 2-form  $\beta = \beta^{xy} dx dy + \beta^{yz} dy dz + \beta^{xz} dx dz$ , where  $\beta^{yz} = \alpha^x$ ,  $\beta^{xz} = -\alpha^y$ ,  $\beta^{xy} = \alpha^z$ . (iii) There do not exist any nonzero harmonic 1-forms in  $\mathbb{R}^3$ .

## References

- [1] Hille B 1992 *Ionic Channels of Excitable Membranes* 2nd edn (Sunderland, MA: Sinauer Associates)
- [2] Hamalainen M, Hari R, Ilmoniemi R J, Knuutila J and Lounasmaa O V 1993 Magnetoencephalography— theory, instrumentation and applications to noninvasive studies of the working human brain *Rev. Mod. Phys.* **65** 413–97
- [3] Clarke J 1994 *SQUIDS Sci. Am.* **271** 46–53
- [4] Geselowitz D B 1970 On the magnetic field generated outside an inhomogeneous volume conductor by internal current sources *IEEE Trans. Magn.* **6** 346–7
- [5] Dassios G and Kariotou F 2003 On the Geselowitz formula in biomagnetics *Quart. Appl. Math.* **61** 387–400
- [6] Grynszpan F and Geselowitz D B 1973 Model studies of the magnetocardiogram *Biophys. J.* **13** 911–25
- [7] Ilmoniemi R J, Hamalainen M S and Knuutila J 1985 The forward and inverse problems in the spherical model *Biomagnetism: Applications and Theory* ed H Weinberg, G Stroink and T Katila (New York: Pergamon)

- 
- [8] Sarvas J 1987 Basic mathematical and electromagnetic concepts of the biomagnetic inverse problem *Phys. Med. Biol.* **32** 11–22
- [9] Helmholtz H 1853 Ueber Einige Gesetze der Vertheilung Elektrischer Strome in Korperlichen Leitern mit Anwendung auf Dietherisch–Elektrischen Versuche *Ann. Phys. Chem.* **89** 211–33  
Helmholtz H 1853 Some laws about the distribution of electrical currents in volume conductors, with application to animal electric experiments *Ann. Phys. Chem.* **89** 353–77
- [10] Ioannides A A, Bolton J P R and Clarke C J S 1990 Continuous probabilistic solutions to the biomagnetic inverse problem *Inverse Problems* **6** 523–42
- [11] See Images of Conflict: MEG vs EEG, by Crease R P 1991 *Science* **253** 374–5
- [12] Dassios G and Kariotou F 2003 Magnetoencephalography in ellipsoidal geometry *J. Math. Phys.* **44** 220–41
- [13] Scherg M 1990 Fundamentals of dipole source potential analysis *Auditory Evoked Magnetic Fields and Electric Potentials (Advances in Audiology vol 6)* ed F Grandori, M Hoke and G L Romani (Basel: Karger) pp 40–69
- [14] DeMunck J C 1990 The estimation of time varying dipoles on the basis of evoked potentials *Electroenceph. Clin. Neurophys.* **77** 156–60
- [15] Hamalainen M S and Ilmoniemi R J 1994 Minimum-norm estimation in a boundary-element torso model *Med. Biol. Eng. Comp.* **32** 43–8
- [16] Fokas A S, Gel'fand I M and Kurylev Y 1996 Inversion method for magnetoencephalography *Inverse Problems* **12** L9–11
- [17] Press W H, Teukolsky S A, Vetterling W T and Flannery B P 1992 *Numerical Recipes in Fortran. The Art of Scientific Computing* 2nd edn (Cambridge: Cambridge University Press)